Unified approach to the linear optical properties of strained $(Si)_n/(Ge)_m$ superlattices

C. Tserbak and G. Theodorou
Department of Physics, Aristotle University of Thessaloniki, 54006 Thessaloniki, Greece
(Received 13 July 1994)

The linear optical properties of $(Si)_n/(Ge)_m$ strained-layer superlattices (SLS's) grown on $Si_{1-x}Ge_x(001)$ substrates are studied within the framework of the tight-binding approximation. A systematic study of the influence of periodicity $(n+m)$, composition (n/m), and strain of the superlattice on the E_1-like and E_2-like transitions of the dielectric function is presented. The near-gap absorption coefficient is calculated and the contribution of the pseudodirect transitions is investigated. The dielectric function $\varepsilon_2(\omega)$ of Si/Ge SLS's is compared with the average crystal dielectric function $\varepsilon_2^a(\omega)$, as well as to the mean value of the dielectric function of the constituent materials, $\varepsilon_2^m(\omega)$. For light polarization parallel to the growth plane, the dielectric functions of the SLS is better described by the $\varepsilon_2^m(\omega)$ spectrum, even for thin SLS's. For polarization along the growth axis it is closer to the $\varepsilon_2^a(\omega)$ spectrum and only for quite thick SLS's do we observe Ge-like and Si-like features. These results are also confirmed with the use of a decomposition technique of the SLS wave function.

I. INTRODUCTION

In the last decade, a large number of theoretical and experimental works on the electronic and optical properties of Si/Ge strained-layer superlattices (SLS's) have appeared in the literature. This is mainly due to the fact that thin Si/Ge SLS's composed of two technologically important indirect-gap semiconductors have the potential of becoming direct-band-gap materials appropriate for use in optoelectronic devices.[1,2] From the theoretical point of view, most of the work on these SLS's has been devoted to electronic-band-structure calculations.[3–11] Methods with various degrees of sophistication have been used for this purpose, i.e., effective-mass Kronig-Penney models, empirical pseudopotentials, empirical tight-binding (ETB) models, self-consistent pseudopotentials, linear-muffin-tin-orbital (LMTO) models, and others. From the experimental point of view, most of the important experiments concern photoreflectance, electroreflectance, and photoluminescence measurements.[12–16] These measurements are particularly sensitive to critical-point transitions but give no information about all other transitions. Recently, measurements of the imaginary part of the dielectric function $\varepsilon_2(\omega)$ as well as the absorption spectra for some Si/Ge SLS's have been reported.[17–21] These spectra give information on transitions in the entire Brillouin zone (BZ). The measured optical spectra possess many structures and for their interpretation detailed theoretical calculations are needed. To our knowledge, only a few theoretical works have been so far devoted to the calculation of the linear optical properties of Si/Ge SLS's.[22–24]

To our knowledge, the first reported calculations of the dielectric functions were done by Ghahramani, Moss, and Sipe.[22] They used an *ab initio* minimal basis of orthogonalized linear combination of Gaussian orbitals technique to produce the band structure of the SLS's. This method, however, does not describe accurately the conduction bands and, in addition, the oscillator strengths are too small. As a result, the calculated dielectric functions deviate considerably from the real ones. Their investigation was mainly limited to the tetragonal anisotropy of these SLS's. At the same time, Gell[23] calculated the adsorption coefficients for the $(Si)_4/(Ge)_4$ SLS grown on different $Si_{1-x}Ge_x$ buffers by means of the empirical pseudopotential method. He found that the absorption spectra near the band gap are different from those of the corresponding alloy. He also predicted quite a strong anisotropy in the spectra and a large influence by the substrate. Schmid, Christensen, and Cardona[24] presented a more complete investigation of the optical properties of Si/Ge SLS's. Their calculations have been performed within the local-density approximation (LDA) by means of the self-consistent relativistic LMTO method. The well-known band-gap problem of the LDA method is corrected by including an external potential in the calculations. This work was limited to a few short period Si/Ge SLS's and mainly to the study of their anisotropy. As in all *ab initio* methods, LMTO becomes computationally very demanding as the SLS period increases. This is especially true for the computation of optical response functions, where integration in the entire BZ is needed. In all the above-mentioned works the spin-orbit coupling has been ignored in the calculations of the optical properties.

Very recently, the present authors reported calculations for the optical absorption of the strain-symmetrized $(Si)_{10-n}/(Ge)_n$ SLS's.[25] The calculations were performed within a reliable and computationally very efficient ETB model,[11] including the spin-orbit interaction, and were limited to the optical transitions near the band gap. Here, we present a systematic theoretical study of the linear optical properties of the Si/Ge SLS's. More specifically, we calculate the complex dielectric function $\varepsilon(\omega)=\varepsilon_1(\omega)+i\varepsilon_2(\omega)$ for a variety of Si/Ge SLS's. The dependence of several structures that appear in the opti-

0163-1829/94/50(24)/18179(10)/$06.00

cal spectra on the buffer alloy $Si_{1-x}Ge_x$ composition, the periodicity $(n+m)$ and the synthesis (n/m) of SLS's is investigated. The imaginary part of the dielectric function $\varepsilon_2(\omega)$ is computed and compared with the average crystal[26] dielectric function $\varepsilon_2^a(\omega)$ as well as with the mean value of the dielectric functions of the constituent materials, $\varepsilon_2^m(\omega)$. The pseudodirect transitions in the low-energy region are also examined and their contribution to the absorption spectra as well as the most important interband contributions are determined.

The paper is organized as follows: In Sec. II, the method for band-structure calculations is briefly described. The method for the calculation of the linear response functions is also presented in the same section. The resulting optical properties of $(Si_n/Ge)_m$ SLS's are presented in Sec. III, with the case of the $(Si)_4/(Ge)_4$ SLS extensively studied. The influence of periodicity $(n+m)$, composition (n/m), and strain on the optical transitions is systematically investigated. The dielectric function of the SLS's is compared with $\varepsilon_2^a(\omega)$ and $\varepsilon_2^m(\omega)$. Finally, a decomposition of the SLS wave function is used to analyze the $\varepsilon_2(\omega)$ spectra of the SLS. In Sec. IV, we summarize our findings and give our conclusions.

II. THE METHOD

The details of our model for the calculation of electronic band structures have been already given in the literature,[11] and we only give here a brief description of the method for the sake of completeness. We use an ETB method within an sp^3 set of orbitals and third-neighbor interactions, in the three-center representation, including spin-orbit coupling. The reliability of this model has been already tested.[11] The imaginary part $\varepsilon_2(\omega)$ of the dielectric function is calculated by using the following relation:[27]

$$\varepsilon_2(\omega)=\frac{4\pi^2e^2}{m^2\omega^2}\sum_{C,V}\int\frac{2}{(2\pi)^3}|\langle\mathbf{k},C|\mathbf{P}\cdot\mathbf{a}|\mathbf{k},V\rangle|^2 \times\delta[E_{CV}(\mathbf{k})-\hbar\omega]d\mathbf{k}\ , \quad (1)$$

where $|\mathbf{k},C\rangle$ and $|\mathbf{k},V\rangle$ stand for the wave functions of the conduction and the valence bands, respectively, and $E_{CV}(\mathbf{k})$ for the energy difference between the conduction (C) and the valence (V) band. $\mathbf{P}$ is the momentum operator and $\mathbf{a}$ the polarization unit vector.

In our ETB scheme the momentum matrix elements are expressed in terms of the Hamiltonian matrix elements and distances between localized orbitals.[28,29] The integration in the BZ has been performed within the linear analytic tetrahedron method by using a uniform mesh of $\mathbf{k}$ points.[30,31] Special care has been exercised to use as many $\mathbf{k}$ points as necessary in order to obtain a good convergence and also obtain fine details of the dielectric function. The superlattice Brillouin zone (SBZ) for $(n+m)/2$ even or odd is given in Fig. 1. The $\varepsilon_2(\omega)$ was calculated for energies up to 10 eV. The real part $\varepsilon_1(\omega)$ is obtained from $\varepsilon_2(\omega)$ by the use of the Kramers-Kronig relations, in which the contribution from energies greater than 10 eV is taken into account by the tail formula $(\beta\hbar\omega)/(\hbar^2\omega^2+\gamma^2)^2$, where γ is equal to 4.5 eV and β is determined by the continuity of $\varepsilon_2(\omega)$ at 10 eV.[32] The absorption coefficient $\alpha(\omega)$ is then obtained by the relation,[27]

$$\alpha(\omega)=\frac{\varepsilon_2(\omega)\omega}{cn(\omega)} \quad (2)$$

with $n(\omega)$ the refraction index and c the light velocity.

III. LINEAR OPTICAL PROPERTIES

A. Dielectric function

The imaginary part of the dielectric function $\varepsilon_2(\omega)$ for the $(Si)_4/(Ge)_4$ SLS grown on a Si(001) substrate is calculated. This SLS belongs to the D_{2h}^5 orthorhombic space group and an anisotropy is expected for light polarization along the three main axes of the crystal. The dominant anisotropy is, of course, relevant to polarizations parallel and normal to the interfaces. The anisotropy in the plane of interfaces is quite small. The results for all three polarizations (ε_2^{xx}, ε_2^{yy}, ε_2^{zz}) are displayed in Fig. 2. We point out that the axes used in the present calculations are produced by a rotation of 45° around the z axis of the system, conventionally used in diamond structure. The contribu-

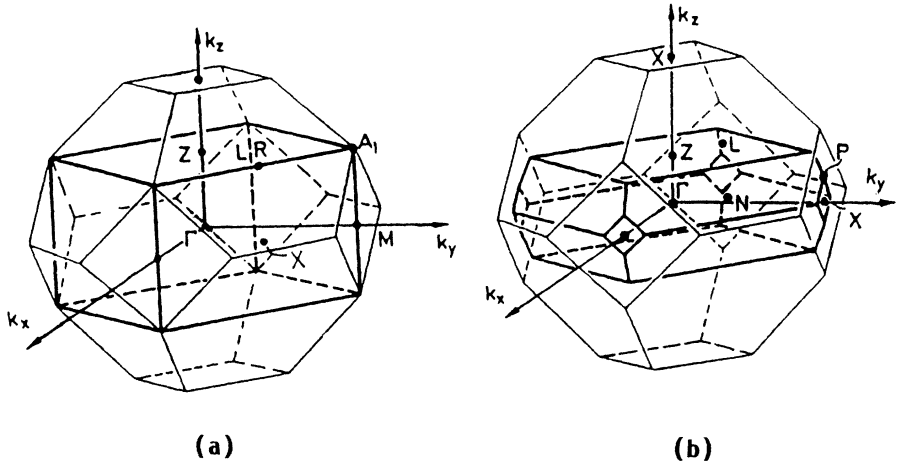

FIG. 1. Brillouin zone for the $(Si)_n/(Ge)_m$ SLS with $(n+m)/2$ (a) even and (b) odd.

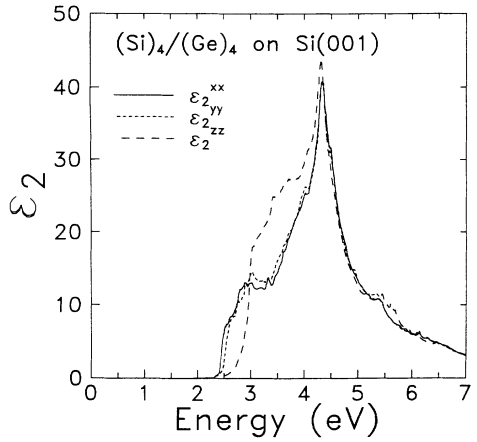

FIG. 2. Imaginary part of the dielectric function $\epsilon_2(\omega)$ for the $(Si)_4/(Ge)_4$ SLS grown on a Si(001) substrate for light polarization along the three main axis.

tions coming from the pseudodirect transitions are not distinguishable in Fig. 2. These contributions are limited in the range from the absorption edge up to about 2.5 eV and produce small values in ε_2. It is well known[11,24] that the pseudodirect transitions are characterized by transition probabilities 2–5 orders of magnitude smaller than the first direct transitions of the average crystal, and their contribution will be examined later. The anisotropy between $\varepsilon_2^{xx}(\varepsilon_2^{yy})$ and ε_2^{zz} is significant in the energy range 2.5–4 eV, and becomes very small above 4 eV. For energies in the range 2.5–3 eV the functions ε_2^{xx} and ε_2^{yy} are greater than ε_2^{zz}, while the opposite is true for energies in the range 3–4 eV. This behavior of anisotropy can mainly be attributed to the tetragonal distortion of Ge layers. As shown in Fig. 2, the anisotropy in the (x,y) plane between ε_2^{xx} and ε_2^{yy} takes appreciable values only in the range between 2.5 and 3.5 eV. This can be explained on the basis of the band structure shown in Fig. 3. In the above-mentioned region, the main contributions to the dielectric function come from transitions that take place around the ΓX_1, ΓX_2, ΓR_1, and ΓR_2 directions of the SBZ. The different dispersion of the bands along these directions results in a relative shift of the position and amplitude of ε_2^{xx} and ε_2^{yy}.

In the spectrum of $\varepsilon_2(\omega)$, Fig. 2, we observe mainly two groups of structures. The first one is located around 3 eV, is relatively spread out, and has its origin in the E_1 transitions of bulk Si and Ge. The second and most pronounced one is around 4.35 eV and comes from the E_2 transitions of the constituent materials. The E_1 and $E_1+\Delta_1$ structures in pure Si and Ge are due to transitions between the two upper valence bands (V_1 and V_2) and the lowest conduction band (C_1) near the L point and along the Λ direction of the BZ and differ appreciably (~ 1.2 eV). In Si/Ge SLS's these transitions split into several components because of zone folding, strain, and the lower symmetry of the SLS's. As a consequence, the E_1-like structure in the SLS dielectric function is relatively broad and is strongly affected by the SLS composition. In the case of $(Si)_4/(Ge)_4$ SLS, the L points of the average crystal BZ are folded to the nonequivalent (because of the orthorhombic symmetry) points X_1 and X_2 of the SBZ. In the E_1-like structure of $\varepsilon_2(\omega)$ we can distinguish transitions at the following energies: 2.54, 2.57, 2.74, 2.93, 3.21, 3.25, 3.27, 3.3, and 3.4 eV. The first four transitions have their origin near the X_1 and X_2 points of the SBZ, while the last two take place along the ΓM direction. The transitions at 3.21, 3.25, and 3.27 eV originate from regions near the R_1 and R_2 points of the SBZ. The most pronounced structure in $\varepsilon_2(\omega)$ is the E_2 peak and appears at 4.35 eV. This is because the E_2 structures of bulk Si and Ge appear at approximately the same energy, 4.35 and 4.4 eV, respectively. This structure comes from a small area around the M point of the SBZ. Besides the main peak, some other weak structures also appear, the most intensive being at energies 4.1 and 4.54 eV.

The strain produced by the buffer on which the SLS's are grown affects significantly the superlattice dielectric function. The dielectric function $\varepsilon_2(\omega)$ of the $(Si)_4/(Ge)_4$ SLS grown on a Ge(001) substrate as well as on $Si_{0.44}Ge_{0.56}$ alloy buffer, are shown in Fig. 4. The latter SLS corresponds to the strain-symmetrized case. We have seen before (Fig. 2) that for growth on a Si(001) substrate and in the energy region of 3–4 eV, $\varepsilon_2^{zz}(\omega)$ is larger

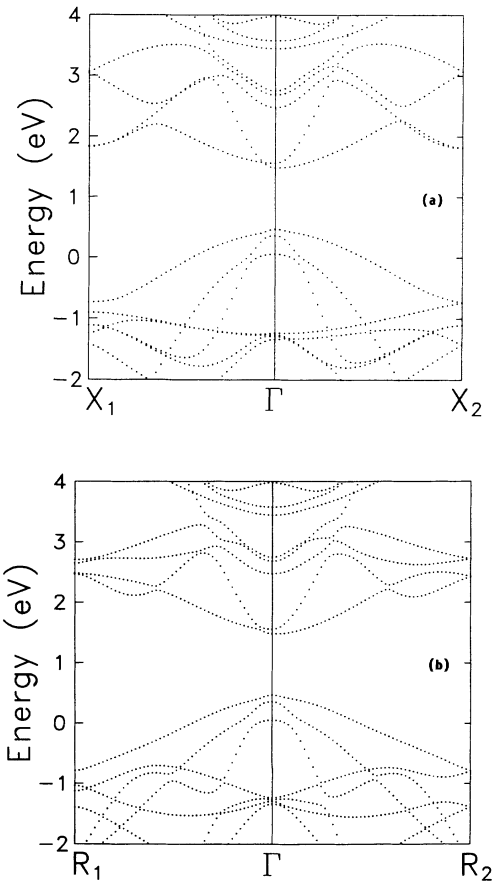

FIG. 3. Energy band structure of the $(Si)_4/(Ge)_4$ SLS grown on a Si(001) substrate, along the symmetry lines (a) ΓX_1, ΓX_2 and (b) ΓR_1, ΓR_2.

than $\varepsilon_2^{xx}(\omega)$ and $\varepsilon_2^{yy}(\omega)$. This behavior is reversed for the case of a Ge(001) substrate. This is mainly due to the uniaxial distortion of the Si layers. For energies larger than 4 eV, the dielectric function is almost isotropic.

The tail in the dielectric function of the $(Si)_4/(Ge)_4$ SLS in the energy range below 2.4 eV becomes more pronounced as the Ge content of the buffer increases. The E_1-like structure for the case of the Ge substrate is composed of a group of transitions, the most intense being at about 2.7 eV. The E_2 peak splits into two components with energies 4.02 and 4.2 eV. By comparing these values of transition energies with the corresponding ones for growth on Si(001), we conclude that generally the critical-point energies shift to lower values as we go from a Si(001) to Ge(001) substrate. We point out that for the strain-symmetrized case the SLS has the smallest anisotropy, which is limited in the energy range of 2.5–3 eV. In this case also the E_2 peak splits into two components, with an energy splitting smaller than the corresponding one for the case of a Ge(001) substrate.

With the use of Kramers-Kronig relations and the tail formula referred in Sec. II, we have calculated the real part of the dielectric function, $\varepsilon_1(\omega)$. The results for the

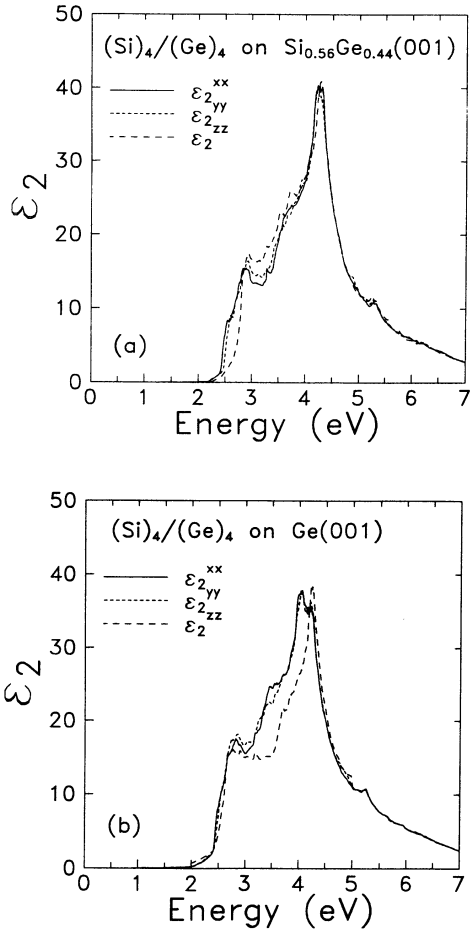

FIG. 4. Imaginary part of the dielectric function $\varepsilon_2(\omega)$ for the $(Si)_4/(Ge)_4$ SLS grown on a (a) $Si_{0.56}Ge_{0.44}$ (001) and (b) Ge(001) substrate, for light polarization along the three main axes.

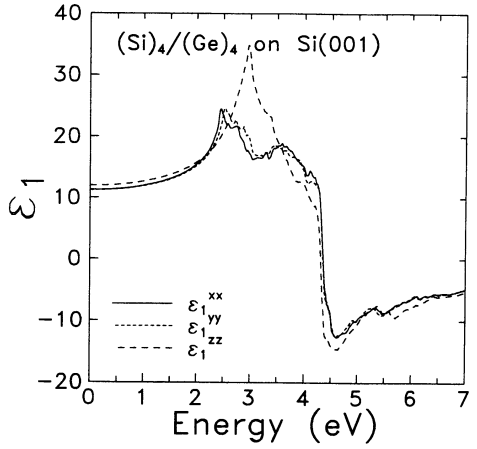

FIG. 5. Real part of the dielectric function $\varepsilon_1(\omega)$ for the $(Si)_4/(Ge)_4$ SLS grown on a Si(001) substrate for light polarization along the three main axes.

$(Si)_4/(Ge)_4$ SLS grown on a Si(001) substrate are shown in Fig. 5. The interband contribution to the static dielectric constant $\varepsilon_0^i(i=\|,\perp)$ can be calculated, by the use of the following relation:[27]

$$\varepsilon_0^i = 1 + \frac{2}{\pi} P \int \frac{\varepsilon_2^i(\omega)}{\omega} d\omega \ . \tag{3}$$

The $(Si)_4/(Ge)_4$ SLS possesses orthorhombic symmetry and, therefore, $\varepsilon_0^{xx} \neq \varepsilon_0^{yy}$. Our calculations show that this difference is very small and will be ignored; instead we will concentrate on the values of $\varepsilon_0^{\|}$ and $\varepsilon_0^{\perp}$. The results for the $(Si)_4/(Ge)_4$ SLS grown on different substrates are displayed in Table I. In the same table the static dielectric constants of the constituent materials are also included. The value of $\varepsilon_0^{\|}$ increases with the increase of the Ge concentration in the alloy buffer, while the opposite occurs for $\varepsilon_0^{\perp}$.

B. Absorption spectra

Up to now, we did not pay attention to the energy region below 2.5 eV, where the pseudodirect transitions dominate. To investigate this region we have calculated

TABLE I. Static dielectric constant of the $Si_4/(Ge)_4$ SLS grown on a (001) surface of Si, $Si_{0.56}Ge_{0.44}$, and Ge substrates. The static dielectric constants of the average crystal (ε_0^a), as well as the mean value of the static dielectric constants of the strained constituent materials of the SLS, are also shown for comparison.

Substrate	Si	$Si_{0.56}Ge_{0.44}$	Ge
$\varepsilon_0^{\|}$	11.26	11.77	12.60
$\varepsilon_0^{\perp}$	11.97	11.63	11.28
$\varepsilon_0^{a\|}$	11.14	11.61	12.02
$\varepsilon_0^{a\perp}$	11.98	11.55	10.88
$\varepsilon_0^{m\|}$	11.54	12.31	13.04
$\varepsilon_0^{m\perp}$	12.22	12.16	11.85

the absorption spectra near the gap of the $(Si)_4/(Ge)_4$ SLS grown on three different substrates (Si, $Si_{0.56}Ge_{0.44}$, and Ge), and for all three polarizations. The results are shown in Fig. 6. From this figure we conclude that the absorption edge moves to lower energies as the concentration x of Ge in the buffer increases. This happens because as the distortion of Si layers increases, the conduction-band minimum, which is mainly determined by Si, lowers its energy. The slope of $\alpha(\omega)$ near the gap increases with the increase of x. The most rapid increase occurs for polarization along the [001] direction. For polarization along the [001] direction we observe a steplike behavior in the absorption spectra, characteristic of a two-dimensional motion.

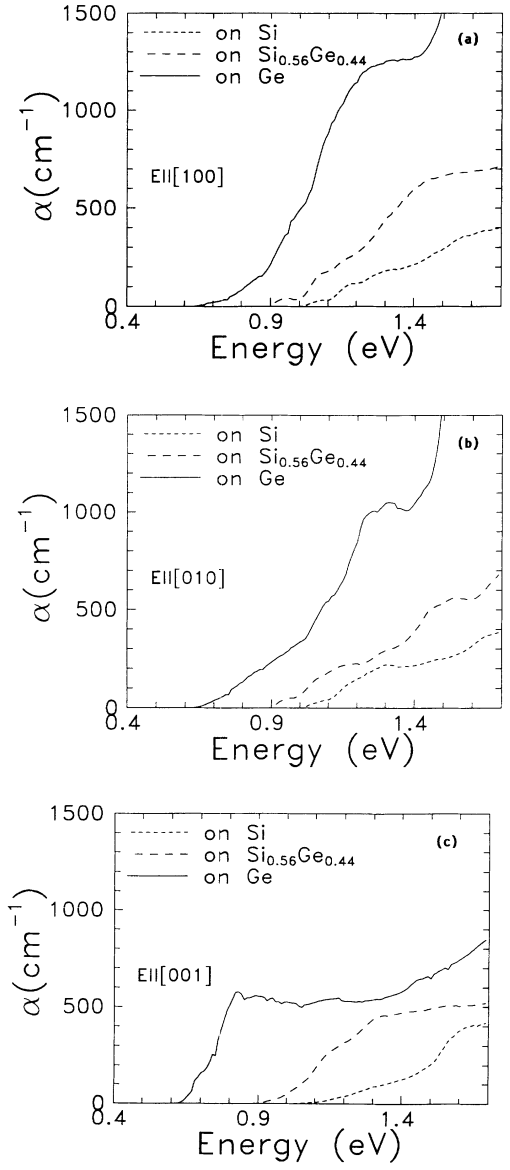

FIG 6. Absorption coefficient for the $(Si)_4/(Ge)_4$ SLS grown on a (001) surface of Si, $Si_{0.56}Ge_{0.44}$, and Ge substrates, for light polarization along the (a) [100], (b) [010], and (c) [001] directions.

According to Eq. (2), the absorption coefficient is proportional to ε_2. Therefore, in order to obtain more information for the transitions responsible for the absorption near the edge, we have decomposed the dielectric function into terms $[\varepsilon_2(\omega)]_{C,V}$, corresponding to transitions between the valence (V) and the conduction (C) band. Then the corresponding contribution to the absorption coefficient is

$$\alpha_{C,V}(\omega)=\frac{[\varepsilon_2(\omega)]_{C,V}\omega}{cn} . \tag{4}$$

In this analysis, only transitions between the three upper valence (V_1-V_3) and the three lower conduction bands (C_1-C_3) were taken into account. By assuming constant momentum matrix elements, $\varepsilon_2(\omega)$ becomes proportional to the joint density of state (JDOS) divided by ω^2. The critical-point structures of $\varepsilon_2(\omega)$ also originates from JDOS/ω^2. In order to separate the contribution of the matrix elements from the density of states, we have calculated JDOS/ω^2. The results are shown in Fig. 7. In the spectrum of JDOS/ω^2 one can discern the critical-point structures which may originate from the Γ and Z points of the SBZ. From the same figure we can deduce that the transition 1-1 (from now on, we will symbolize the transitions V_i-C_j with $i-j$) contributes the most to JDOS/ω^2, while transitions 3-1 and 3-2 contribute much less. This is because V_1 and C_1 bands have small dispersion in the ΓZ direction, while the V_3 valence band has a larger dispersion in the same direction.

In addition to JDOS/ω^2 we have also calculated the transition matrix elements $|M_{C,V}(\mathbf{k})|^2 = |\langle \mathbf{k},C|\mathbf{P}\cdot\mathbf{a}|\mathbf{k},V\rangle|^2$, for all three polarizations, as a function of the wave vector along the ΓZ direction. The results are displayed in Fig. 8. From this figure we conclude that for polarization in the growth plane the strongest transitions are 1-2 and 2-2. Their probabilities decrease as the distance from the center of the BZ becomes larger. Transitions 3-1 and 3-2 are characterized by very small transition probabilities and depend very little on the wave vector. For polarization along the [001]

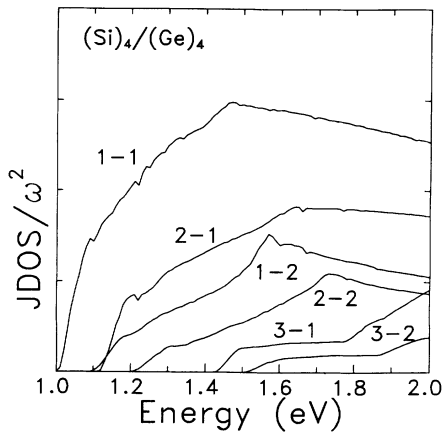

FIG. 7. Contribution of the interband transitions $i-j$, with $i=1,2,3$ and $j=1,2$, to the quantity JDOS/ω^2 for the $(Si)_4/(Ge)_4$ SLS grown on a Si(001) substrate.

direction this behavior is reversed. Now transitions 3-1 and 3-2 have the largest transition probabilities while the rest are characterized by very small probabilities. Figure 9 shows the contributions to $\alpha(\omega)$ of the transitions between the top three valence bands and the lower three conduction bands to $\alpha(\omega)$ for light polarization parallel to x,y, and z directions. For energies smaller than 2 eV the transitions that contribute almost exclusively to $\alpha(\omega)$ are between the two upper valence and the two lower conduction bands. These transitions take place in an area around the ΓZ direction of the SBZ. For (x,y) polarization the contribution to $\alpha(\omega)$ from the lowest interband transitions (1-1, 1-2, 2-1, 2-2) increases rapidly near the corresponding absorption edges. For [100] polarization the most important contribution to $\alpha(\omega)$ comes from the 1-2 transition, while for [010] polarization comes from the 1-1 transition. For light polarization parallel to the [001] direction, the behavior of the first four components of $\alpha(\omega)$ near the corresponding gaps is almost linear.

C. Mean value and average crystal dielectric functions

To further analyze the dielectric function of the $(Si)_4/(Ge)_4$ SLS grown on Si(001), we are going to com-

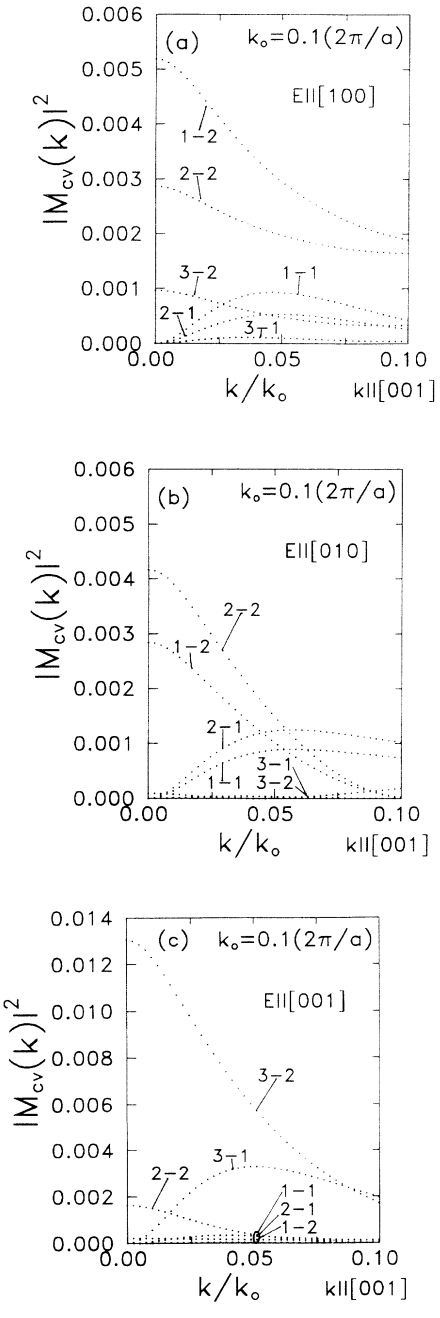

FIG. 8. Transition matrix elements in units of $(h/a_{Si})^2$, for the $(Si)_4/(Ge)_4$ SLS grown on Si, plotted as a function of the wave vector along the ΓZ direction, for light polarization along the (a) [100], (b) [010], and (c) [001] directions.

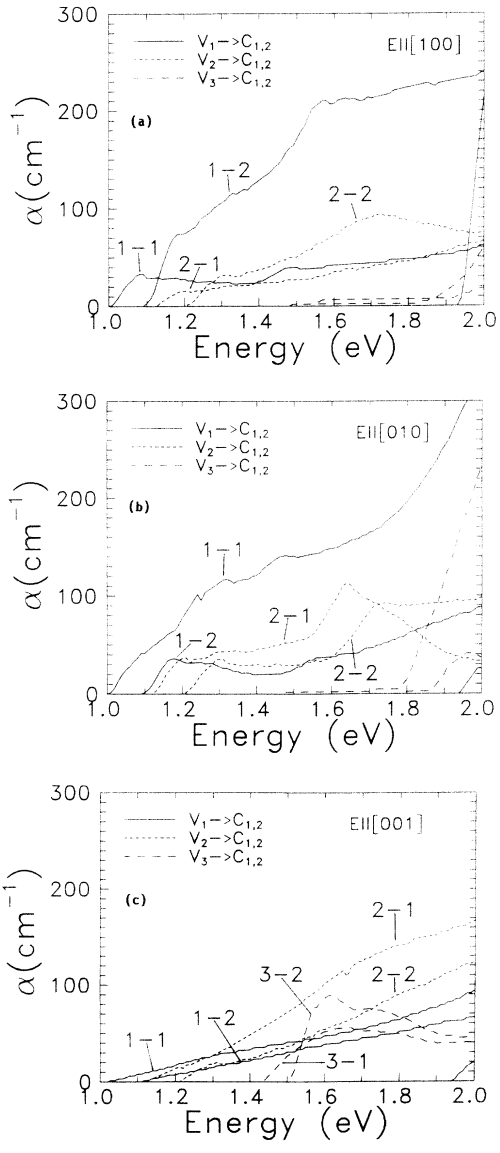

FIG. 9. Contribution to the absorption coefficient from the optical transitions between the $V_{1,2,3}$ and $C_{1,2,3}$ bands for the $(Si)_4/(Ge)_4$ SLS grown on Si(001) and light polarization along (a) [100], (b) [010], and (c) [001] directions.

pare it with the dielectric function of the average crystal,[26] $\varepsilon_2^a(\omega)$, as well as with the mean value of the dielectric functions of cubic Si and tetragonally distorted Ge coherently grown on a Si(001) surface, $\varepsilon_2^m(\omega)$. This comparison for polarization parallel and perpendicular to the interface plane is shown in Fig. 10. In this comparison, the in-plane anisotropy is neglected, and instead the value $\varepsilon_2^{\parallel}(\omega)=[\varepsilon_2^{xx}(\omega)+\varepsilon_2^{yy}(\omega)]/2$ is used. We see that for light polarization parallel to the interface plane the dielectric function of the SLS is closer to $\varepsilon_2^m(\omega)$ than to $\varepsilon_2^a(\omega)$. This is because for this polarization, the electric field causes motion of electrons in the layers of Si and Ge, and consequently the system behaves as a superposition of two independent materials. The tail in $\varepsilon_2^m(\omega)$, below 2.3 eV, does not appear in the dielectric function of the SLS and originates from the distorted Ge layers. Quite thick SLS's are needed in order to obtain it in their spectra. Another important conclusion deduced from Fig. 10 is that the E_2 peaks in $\varepsilon_2^a(\omega)$ and $\varepsilon_2^m(\omega)$ spectra almost coincide. This is explained by the fact that the E_2 structures in Si and tetragonally strained Ge appear at very close energies. However, despite the gross similarities between the dielectric function $\varepsilon_2^{\parallel}(\omega)$ of the SLS and $\varepsilon_2^m(\omega)$, $\varepsilon_2^{\parallel}(\omega)$ possesses many more structures that do not appear in either $\varepsilon_2^a(\omega)$ or $\varepsilon_2^m(\omega)$ spectra. For light polarization perpendicular to the interface, the SLS dielectric function $\varepsilon_2^{\perp}(\omega)$ is closer to $\varepsilon_2^a(\omega)$. For this polarization, the electric field causes the electrons to move into both Si and Ge layers and consequently they feel the potential of an average material, i.e., the average crystal potential. The static dielectric constants for the average crystal as well as the mean value of the constituent materials, $\varepsilon_0^{a\parallel}$, $\varepsilon_0^{a\perp}$, $\varepsilon_0^{m\parallel}$, and $\varepsilon_0^{m\perp}$, and their dependence on the buffer alloy are shown in Table I. From this table we conclude that the average crystal approximates better the values of the static dielectric constants of the SLS than the mean value for the constituent materials.

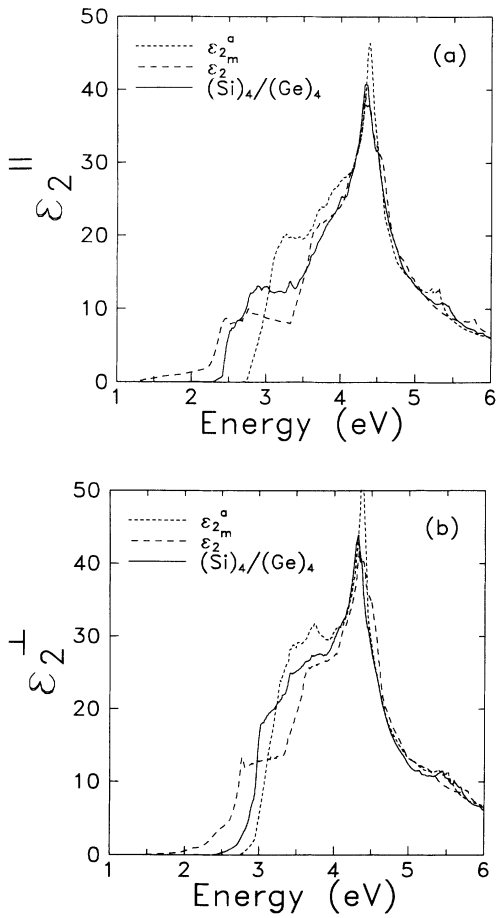

FIG. 10. Dielectric function $\varepsilon_2(\omega)$ of the $(Si)_4/(Ge)_4$ SLS grown on a Si(001) substrate, dielectric function of the corresponding average crystal $\varepsilon_2^a(\omega)$ and the mean value of the dielectric functions of bulk Si and tetragonally distorted Ge grown on Si(001), $\varepsilon_2^m(\omega)$. The results are shown for two polarizations: (a) parallel and (b) perpendicular to the interface plane.

D. Influence of superlattice periodicity and composition

The lattice period and composition of a SLS influence its optical properties. For the investigation of the dependence of the latter on the period of the superlattice, we have calculated the $\varepsilon_2(\omega)$ spectrum for the strain-symmetrized $(Si)_2/(Ge)_2$, $(Si)_6/(Ge)_6$, and $(Si)_{10}/(Ge)_{10}$ SLS's and compared it with the corresponding dielectric functions $\varepsilon_2^a(\omega)$ and $\varepsilon_2^m(\omega)$. The calculations were performed for two polarizations, parallel and perpendicular to the growth plane (001). The results are shown in Fig. 11.

For polarization parallel to the interface, the dielectric functions of $(Si)_6/(Ge)_6$ and $(Si)_{10}/(Ge)_{10}$ SLS's are very close to the $\varepsilon_2^m(\omega)$ spectrum, while for the extremely thin $(Si)_2/(Ge)_2$ SLS it is better approximated by $\varepsilon_2^a(\omega)$. Thus, with the exception of extremely thin SLS's, for light polarization parallel to the interface plane the mean value of the dielectric functions of the constituent materials, $\varepsilon_2^m(\omega)$, constitutes quite a good approximation to the $\varepsilon_2(\omega)$ spectra of the SLS. As a result, Si-like and Ge-like features appear in the dielectric function of the SLS for this polarization. On the other hand, for polarization along the growth axis, the dielectric functions of thin SLS's are fairly close to the dielectric function of the average crystal, $\varepsilon_2^a(\omega)$. However, as the period of the SLS becomes larger, $\varepsilon_2(\omega)$ gradually approaches the $\varepsilon_2^m(\omega)$ spectrum. Therefore, for this polarization, only for quite thick SLS's do we observe Si-like and Ge-like features in $\varepsilon_2(\omega)$. These results are in agreement to those found in Sec. III C.

As we have previously mentioned, we distinguish mainly two groups of structures in the $\varepsilon_2(\omega)$ spectra of SLS's, having their origins in the corresponding structures of the bulk materials. The relatively broad and complicated region of the E_1 transitions and the acute peak of the E_2 transitions. In addition to these bulklike transitions we observe a multitude of weak structures originating from zone-folded bands in the SLS. It is very difficult to compare the E_1 transitions of SLS's with different periods and compositions because of the complicated nature of this structure. In a general statement we can say that for both polarizations the main E_1 com-

ponent remains almost unaffected by the SLS period. For the E_2 peak the situation is much simpler. By taking the second derivative spectrum of $\varepsilon_2(\omega)$ we observe a splitting of this peak into two main components, namely E_2^I and E_2^{II}. The energy position is essentially the same as the period of SLS's changes. In particular, the E_2^{II} transition remains essentially unchanged, with energy ~ 4.32 eV, while the energy of the E_2^I transition increases slightly with period and takes the value of ~ 4.22 eV for the $(Si)_{10}/(Ge)_{10}$ SLS.

For the investigation of the influence of the composition (n/m) of the $(Si)_n/(Ge)_m$ SLS on the optical response, we have calculated the dielectric function $\varepsilon_2(\omega)$ for the strain-symmetrized $(Si)_3/(Ge)_7$, $(Si)_4/(Ge)_6$, $(Si)_5/(Ge)_5$, $(Si)_6/(Ge)_4$, and $(Si)_7/(Ge)_3$ SLS's, having $n+m=10$. Their spectra $\varepsilon_2(\omega)$ are shown in Fig. 12. From these spectra it is clear that the group of E_1 transitions (which occur in the energy region 2.5–3.5 eV) depend strongly on the exact composition of the SLS. This can be mainly attributed to the fact that the E_1 transitions of bulk Si and Ge differ significantly. As the number of Si monolayers in the unit cell increases, these transitions are shifted to larger energies, and become more Si-like. From Fig. 12 it is also deduced that the onset of $\varepsilon_2(\omega)$ moves to lower energies as the number of Ge monolayers in the SLS unit cell increases. For the $(Si)_7/(Ge)_3$ SLS takes the value 2.5 eV and reduces to 1.7 eV for the $(Si)_3/(Ge)_7$ SLS.

As far as the E_2 peak is concerned, a change in the

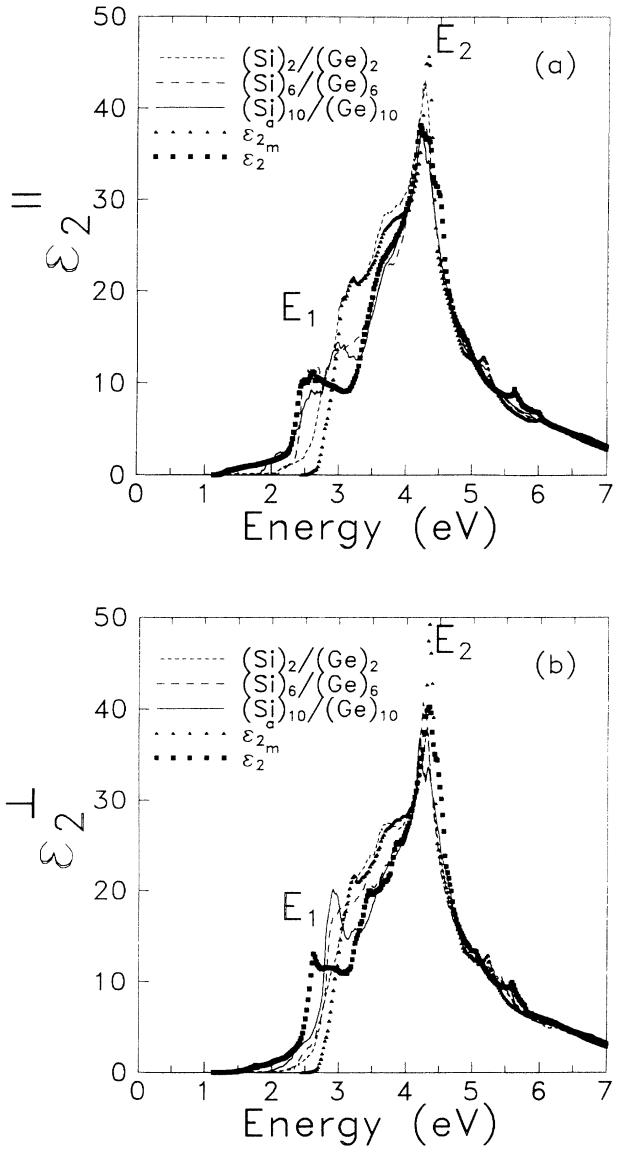

FIG. 11. Dielectric function $\varepsilon_2(\omega)$ of the strain-symmetrized $(Si)_2/(Ge)_2$, $(Si)_6/(Ge)_6$, and $(Si)_{10}/(Ge)_{10}$ SLS compared with the corresponding dielectric functions $\varepsilon_2^a(\omega)$ and $\varepsilon_2^m(\omega)$. Comparison was made for two polarizations, (a) parallel and (b) perpendicular to the interface plane.

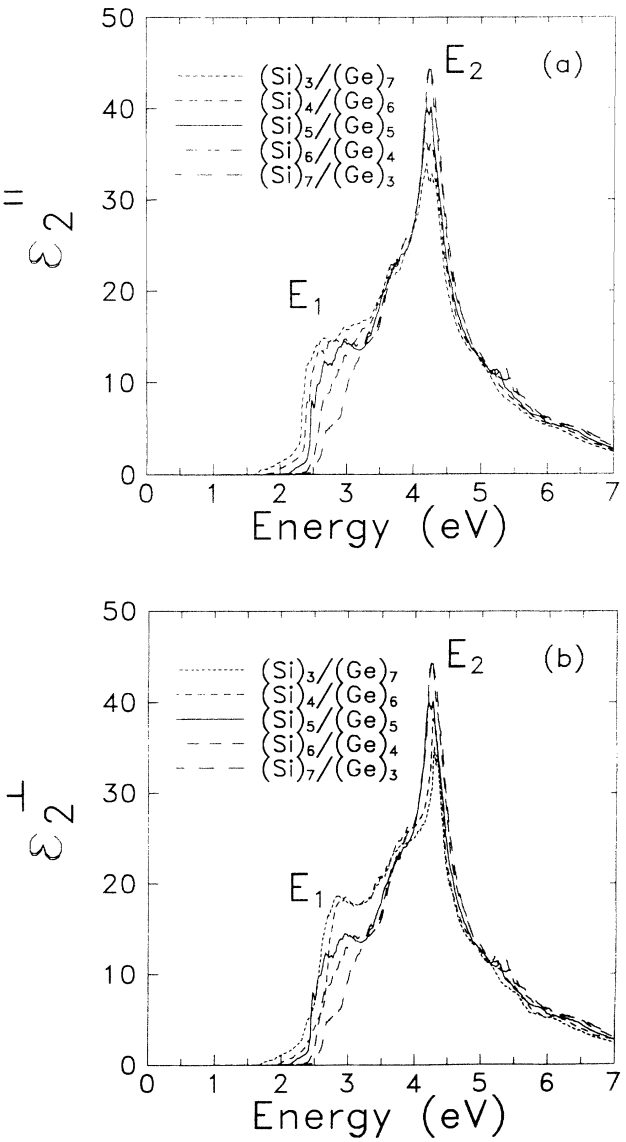

FIG. 12. Dielectric function $\varepsilon_2(\omega)$ of the strain-symmetrized $(Si)_{10-n}/(Ge)_n$ SLS's with $n=3$–7, and light polarization (a) parallel and (b) perpendicular to the interface plane.

composition of the SLS does not alter its energy position, which remains almost constant at an energy of ~4.35 eV. Again, two main components are observed in the E_2 peak that differ by ~0.1 eV. With the increase of the number of Ge monolayers in the SLS unit cell we observe an oscillator strength transfer from the E_2 peak to the E_1-like group of transitions and as a consequence an amplitude reduction of the E_2 peak.

E. Decomposition of the $\varepsilon_2(\omega)$

In a recent work, a decomposition scheme for the SLS wave function has been proposed,[33] in order to extract information for the origin of the structures that appear in their dielectric function. This technique has been applied to the $(Si)_n/(Ge)_n$ SLS's with $n=4$ and 6. The $\varepsilon_2(\omega)$ spectra has been calculated with an ETB method with an sp^3s^* set of orbitals in the two-center approximation and nearest-neighbor interactions.[33] This method provides reliable results only close to the gap. In the present work we are going to use our ETB method and extend this decomposition procedure to the whole energy range.

In this decomposition technique the SLS wave functions, Ψ_k^{SLS}, is decomposed in two parts, one that contains the orbitals localized on Si, and the other on Ge atoms

$$\Psi_{\mathbf{k}}^{SLS}=\Psi_{\mathbf{k}}^{Si}+\Psi_{\mathbf{k}}^{Ge} . \tag{5}$$

Then the momentum matrix elements for transitions between a valence and a conduction band will be written as

$$\langle \Psi_{\mathbf{k},C}^{SLS}|\mathbf{P}\cdot\mathbf{a}|\Psi_{\mathbf{k},V}^{SLS}\rangle=\sum_{i,j}\langle \Psi_{\mathbf{k},C}^{i}|\mathbf{P}\cdot\mathbf{a}|\Psi_{\mathbf{k},V}^{j}\rangle , \tag{6}$$

with i,j = Si, Ge, and the transition probability $|\langle\Psi|\mathbf{P}\cdot\mathbf{a}|\Psi\rangle|^2$ will be decomposed into ten terms, the most important being the Si-Si and Ge-Ge ones,

$$|P_{\text{Si-Si}}^{a}|^2=|\langle \Psi_{\mathbf{k},C}^{Si}|\mathbf{P}\cdot\mathbf{a}|\Psi_{\mathbf{k},V}^{Si}\rangle|^2 \tag{7}$$

and

$$|P_{\text{Ge-Ge}}^{a}|^2=|\langle \Psi_{\mathbf{k},C}^{Ge}|\mathbf{P}\cdot\mathbf{a}|\Psi_{\mathbf{k},V}^{Ge}\rangle|^2 . \tag{8}$$

In Fig. 13 the decomposition of the $\varepsilon_2(\omega)$ for the strain-symmetrized $(Si)_4/(Ge)_4$, $(Si)_5/(Ge)_5$, and $(Si)_8/(Ge)_8$ SLS's into Si-Si and Ge-Ge parts for parallel and perpendicular polarization is presented. For polarization parallel to the interfaces the two main contributions (Si-Si and Ge-Ge components) show similar behavior and are reminiscent of the dielectric function of the constituent materials. For perpendicular polarization and thin SLS's, e.g., $(Si)_4/(Ge)_4$, and $(Si)_5(Ge)_5$, the two main components show behavior similar to the corresponding average crystal, see Fig. 11(b), while for thicker SLS's, e.g., $(Si)_8/(Ge)_8$, approach the dielectric function of the constituent materials.

IV. SUMMARY AND CONCLUDING REMARKS

We have presented a systematic study of the linear optical properties of $(Si)_n/(Ge)_m$ SLS's grown on $Si_{1-x}Ge_x(001)$ buffer alloys. The influence of the period $(n+m)$, composition (n/m), and strain on the optical

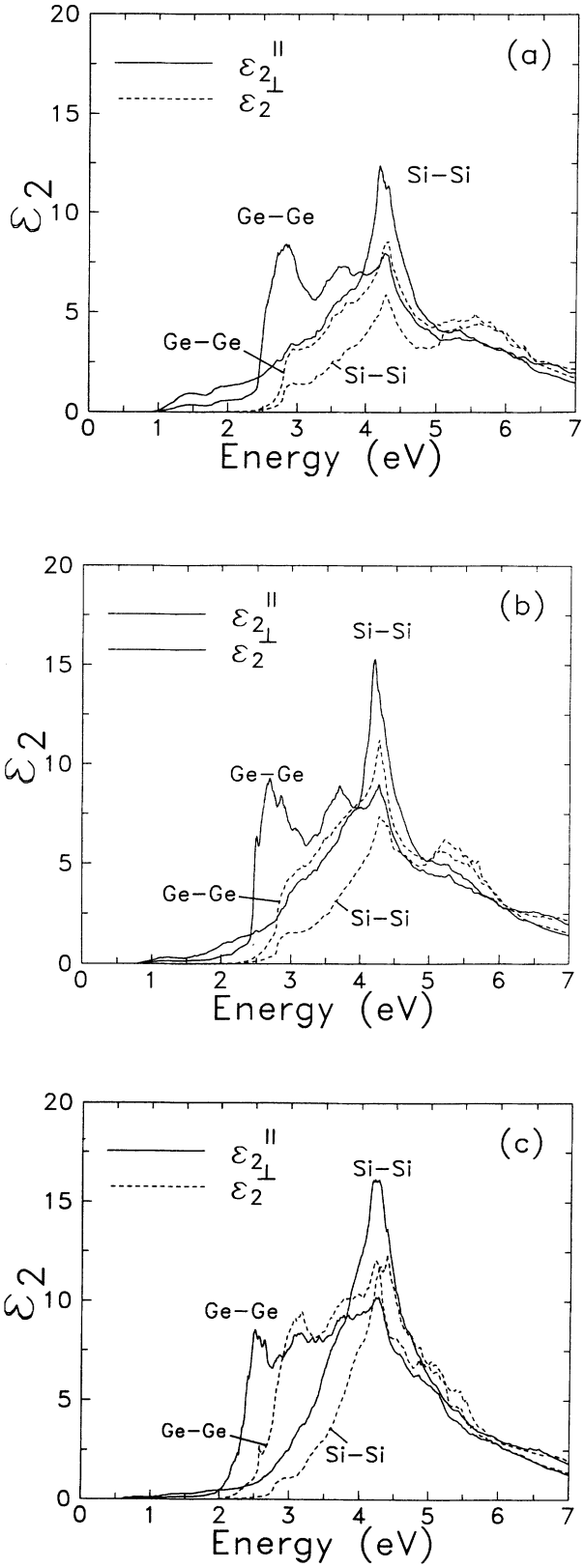

FIG. 13. Decomposition of the imaginary part of the dielectric function into Si-Si and Ge-Ge components for the strain-symmetrized (a) $(Si)_4/(Ge)_4$, (b) $(Si)_5/(Ge)_5$, and (c) $(Si)_8/(Ge)_8$ SLS's, and polarization parallel and perpendicular to the growth plane.

properties of these SLS's has been investigated. The $\varepsilon_2(\omega)$ spectra of the SLS's possess mainly two groups of structures. The first one is located around 3 eV, is relatively broad and it comes from the corresponding E_1 structures of the constituent materials. This structure has many components, and depends strongly on strain and composition. The second and most pronounced structure, around 4.35 eV, originates from the E_2 structures of the constituent materials that appear at approximately the same energy. This explains the acute E_2 peak in $\varepsilon_2(\omega)$ spectra of the SLS. This peak splits into two main components, which are almost unaffected by periodicity, composition, and strain.

We have also compared the dielectric function of Si/Ge SLS's with the average crystal dielectric function $\varepsilon_2^a(\omega)$, and with the mean value of the dielectric functions of the corresponding strained constituent materials, $\varepsilon_2^m(\omega)$. It was found that for light polarized in the growth plane the dielectric functions of the SLS's is better described by the $\varepsilon_2^m(\omega)$ spectrum, even for thin SLS's while for light polarization perpendicular to the growth plane it is closer to the $\varepsilon_2^a(\omega)$ spectrum. The dielectric function is also analyzed in Si-Si and Ge-Ge components.

The case of the $(Si)_4/(Ge)_4$ SLS has been thoroughly studied. The dielectric functions $\varepsilon_2(\omega)$ and $\varepsilon_1(\omega)$ has been calculated and the anisotropy along the three main axes has been investigated. In addition, the absorption spectra near the gap and the contribution of the lowest transitions has been analyzed.

ACKNOWLEDGMENTS

This work was supported in part by the Greek General Secretariat for Research and Technology and the ESPRIT Basic Research Action No. 7128.

[1]T. P. Pearsall, *Critical Reviews in Solid State and Materials Science* (CRC, Cleveland, 1989), Vol. 15, p. 551.
[2]H. Presting, H. Kibbel, M. Jaros, R. M. Turton, U. Menczigar, G. Abstreiter, and H. G. Grimmeiss, Semicond. Sci. Technol. **7**, 1127 (1992).
[3]L. Brey and C. Tejedor, Phys. Rev. Lett. **59**, 1022 (1987).
[4]S. Froyen, D. M. Wood, and A. Zunger, Phys. Rev. B **36**, 4547 (1987); **37**, 6893 (1988).
[5]S. Satpathy, R. M. Martin, and C. G. Van de Walle, Phys. Rev. B **38**, 13 237 (1988).
[6]S. Ciraci and P. I. Batra, Phys. Rev. B **38**, 1835 (1988).
[7]K. B. Wong, M. Jaros, I. Morrison, and J. P. Hagon, Phys. Rev. Lett. **60**, 2221 (1988).
[8]M. A. Gell, Phys. Rev. B **38**, 7535 (1988); **40**, 1966 (1989).
[9]P. Friedel, M. S. Hybertsen, and M. Schluter, Phys. Rev. B **39**, 7974 (1989).
[10]C. Tserbak, H. M. Polatoglou, and G. Theodorou, Europhys. Lett. **18**, 451 (1992).
[11]C. Tserbak, H. M. Polatoglou, and G. Theodorou, Phys. Rev. B **47**, 7104 (1993).
[12]T. P. Pearsall, J. Bevk, L. C. Feldman, J. M. Bonar, J. P. Mannaerts, and A. Ourmazd, Phys. Rev. Lett. **58**, 729 (1987).
[13]T. P. Pearsall, J. M. Vandenberg, R. Hull, and J. M. Bonar, Phys. Rev. Lett. **63**, 2104 (1989).
[14]K. Asami, K. Miki, K. Sakamoto, and S. Gonda, Jpn. J. Appl. Phys. **29**, L381 (1990).
[15]R. Zachai, K. Eberl, G. Abstreiter, E. Kasper, and H. Kibbel, Phys. Rev. Lett. **64**, 1055 (1990).
[16]Y. Yin, D. Yan, F. H. Pollak, M. S. Hybertsen, J. M. Vandenberg, and J. C. Bean, Phys. Rev. B **44**, 5955 (1991).
[17]U. Schmid, F. Lukes, N. E. Christensen, M. Alouam, M. Cardona, E. Kasper, H. Kibbel, and H. Presting, Phys. Rev. Lett. **65**, 1933 (1990).
[18]U. Schmid, J. Humlicek, F. Lukes, M. Cardona, H. Presting, H. Kibbel, E. Kasper, K. Eberl, W. Wegscheider, and G. Abstreiter, Phys. Rev. B **45**, 6793 (1992).
[19]M. S. Hybertsen, M. Schluter, R. People, S. A. Jackson, D. V. Lang, T. P. Pearsall, J. C. Bean, J. M. Vandenberg, and J. Bevk, Phys. Rev. B **37**, 10 195 (1988).
[20]J. Olajos, J. Engvall, H. G. Grimmeiss, H. Kibbel, E. Kasper, and H. Presting, Thin Solid Films **222**, 243 (1992).
[21]U. Menczigar, J. Brunner, E. Friess, M. Gail, G. Abstreiter, H. Kibbel, H. Presting, and E. Kasper, Thin Solid Films **222**, 227 (1992).
[22]E. Ghahramani, D. J. Moss, and J. E. Sipe, Phys. Rev. B **41**, 5112 (1990); **42**, 9193(E) (1990).
[23]M. A. Gell, Semicond. Sci. Technol. **5**, 449 (1990).
[24]U. Schmid, N. E. Christensen, and M. Cardona, Phys. Rev. B **43**, 14 597 (1991).
[25]C. Tserbak and G. Theodorou, Semicond. Sci. Technol. **9**, 1363 (1994).
[26]C. Tserbak, H. M. Polatoglou, and G. Theodorou, Phys. Rev. B **45**, 4327 (1992).
[27]F. Wooten, *Optical Properties of Solids* (Academic, New York, 1972).
[28]N. V. Smith, Phys. Rev. B **19**, 5019 (1979).
[29]L. Brey and C. Tejedor, Solid State Commun. **48**, 403 (1983).
[30]O. Jepsen and O. K. Andersen, Solid State Commun. **9**, 1763 (1971).
[31]G. Lehmann and M. Tauc, Physica Status Solidi B **54**, 469 (1972).
[32]Y. Petroff, M. Balkanski, J. P. Walter, and M. L. Cohen, Solid State Commun. **7**, 459 (1968).
[33]C. Tserbak, H. M. Polatoglou, and G. Theodorou, Phys. Rev. B **44**, 3467 (1992).